Supplemental Figure 1.

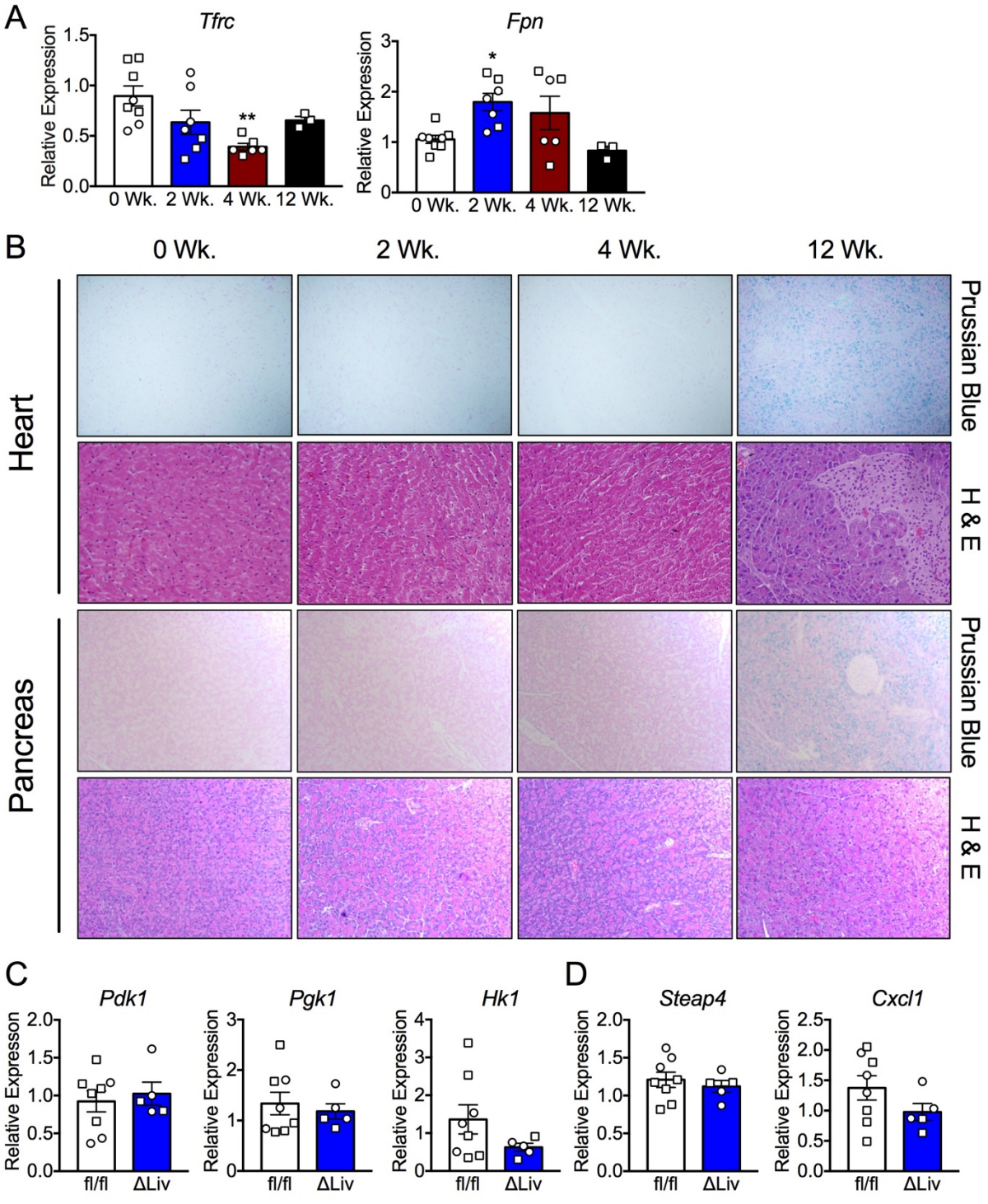

Supplemental Figure 1. Temporal deletion of liver hepcidin alters iron homeostasis and does not affect intestinal HIF-1α target genes or HIF-2α inflammatory targets. (**A**) qPCR analysis of transferrin receptor (*Tfrc*) and ferroportin (*Fpn*) in livers of $Hamp^{\Delta Liv}$ mice (n = 3 to 8 per group). (**B**) Representative Prussian blue iron stain and H&E analysis of hearts and pancreata from $Hamp^{\Delta Liv}$ mice. Images, 20x (n = 3 per group). (**C**) qPCR analysis for HIF-1α-specific transcripts in duodenal samples two-weeks after tamoxifen injection in $Hamp^{fl/fl}$ and $Hamp^{\Delta Liv}$ mice (n = 5 to 8 per group). (**D**) qPCR analysis for HIF-2α-specific inflammatory transcripts in duodenal samples two-weeks after tamoxifen injection in $Hamp^{fl/fl}$ and $Hamp^{\Delta Liv}$ mice (n = 5 to 8 per group). Male samples are designated as squares and female samples are designated as circles. Mean ± SEM are plotted. Significance determined using either one-way ANOVA with Tukey's post hoc (**A**) or 2-tailed unpaired t test (**C** and **D**). *$p < 0.05$; **$p < 0.01$ compared to $Hamp^{fl/fl}$ group.

Supplemental Figure 2.

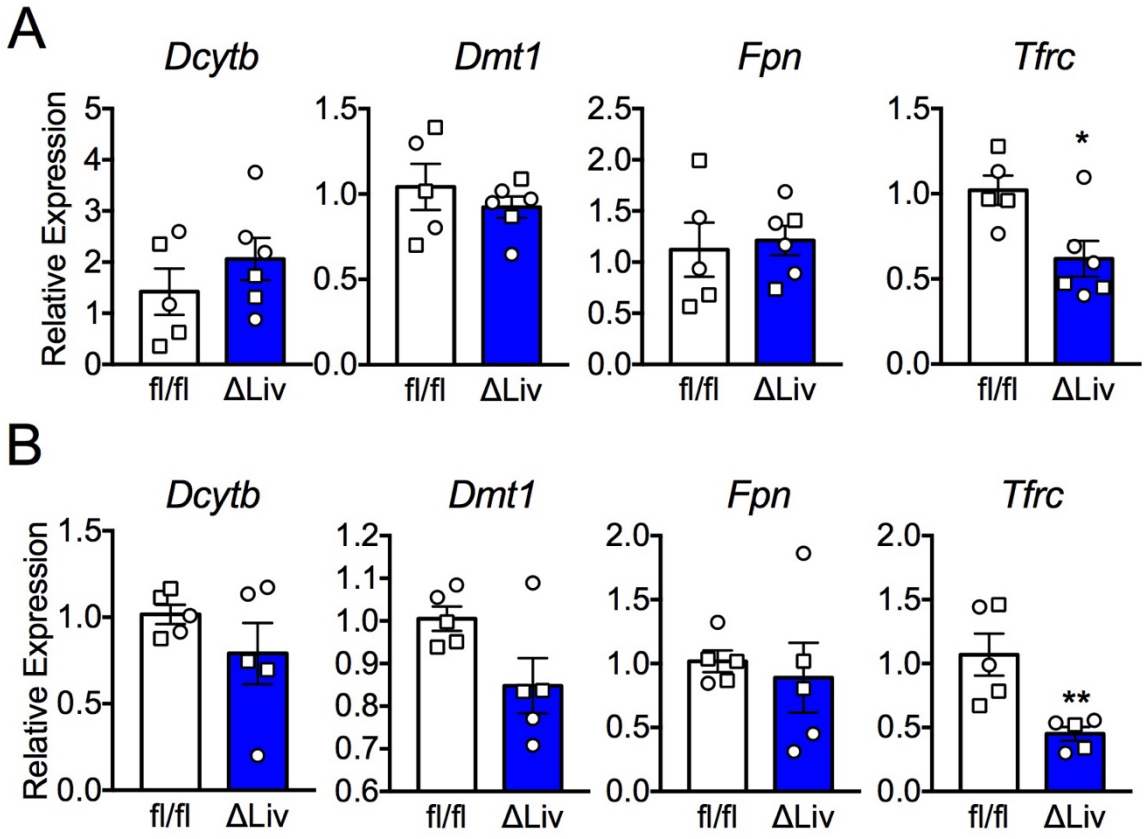

Supplemental Figure 2. Inducible deletion of liver hepcidin does not affect HIF-2α-specific genes in the kidney and spleen. (**A** and **B**) qPCR analysis for HIF-2α-specific and iron handling genes in kidney (**A**) and spleen (**B**) samples of *Hamp*$^{fl/fl}$ and *Hamp*$^{\Delta Liv}$ mice (n = 5 to 6 per group). Male samples are designated as squares and female samples are designated as circles. Mean ± SEM are plotted. Significance determined using 2-tailed unpaired t test. *p < 0.05; **p < 0.01 compared to *Hamp*$^{fl/fl}$ group.

Supplement Figure 3

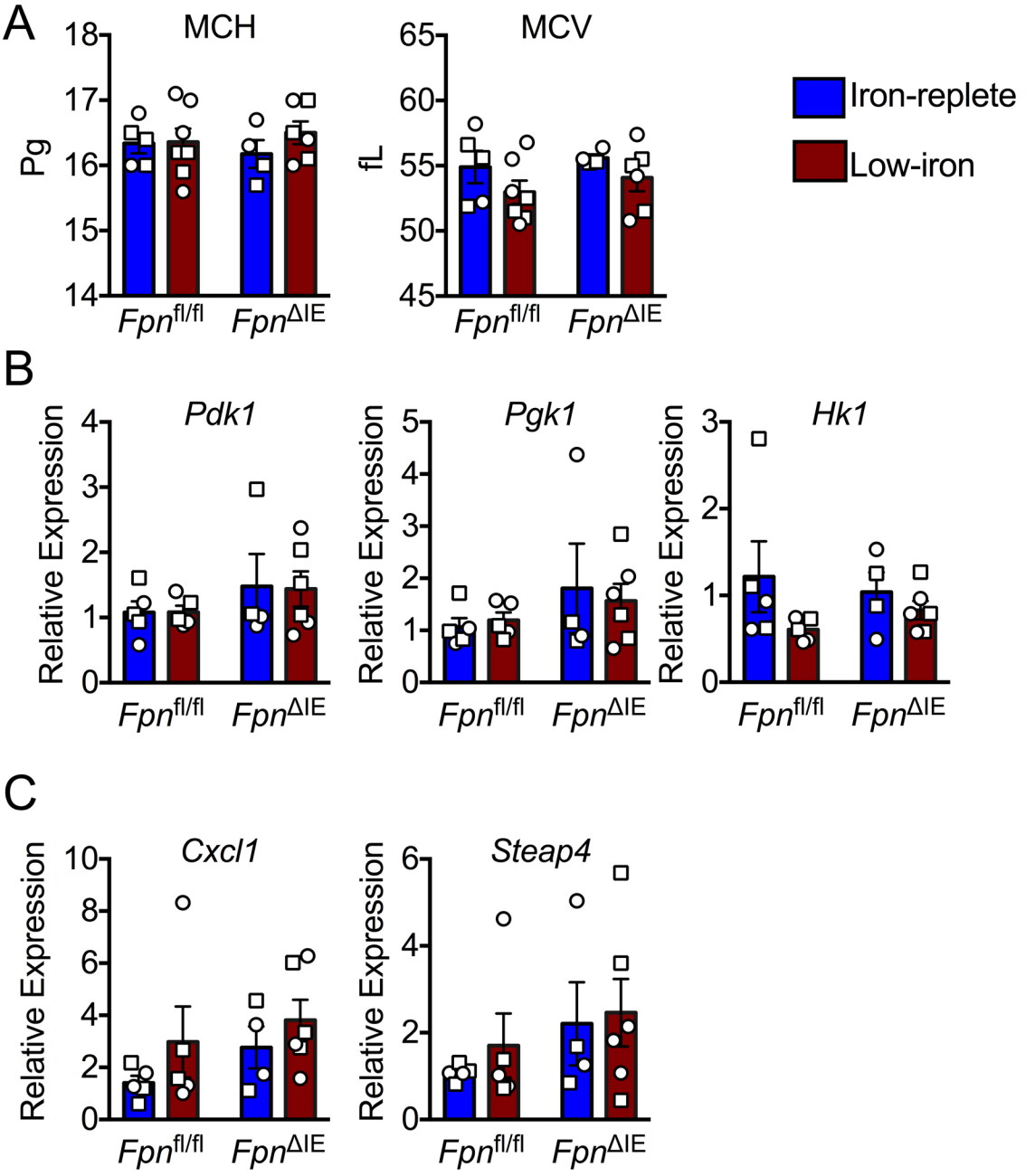

Supplemental Figure 3. The response of intestinal epithelial FPN to systemic iron deficiency does not activate intestinal HIF-1α or HIF-2α inflammatory targets. (**A**) Analysis of mean corpuscular hemoglobin (MCH) and mean corpuscular volume (MCV) (n = 4 to 7 per group). (**B**) qPCR analysis for HIF-1α-specific transcripts in duodenal samples (n = 4 to 6 per group). (**C**) qPCR analysis for HIF-2α-specific inflammatory transcripts in duodenal samples (n = 3 to 6 per group). Male samples are designated as squares and female samples are designated as circles. Mean ± SEM are plotted. Significance determined using two-way ANOVA with Tukey's post hoc.

Supplemental Figure 4.

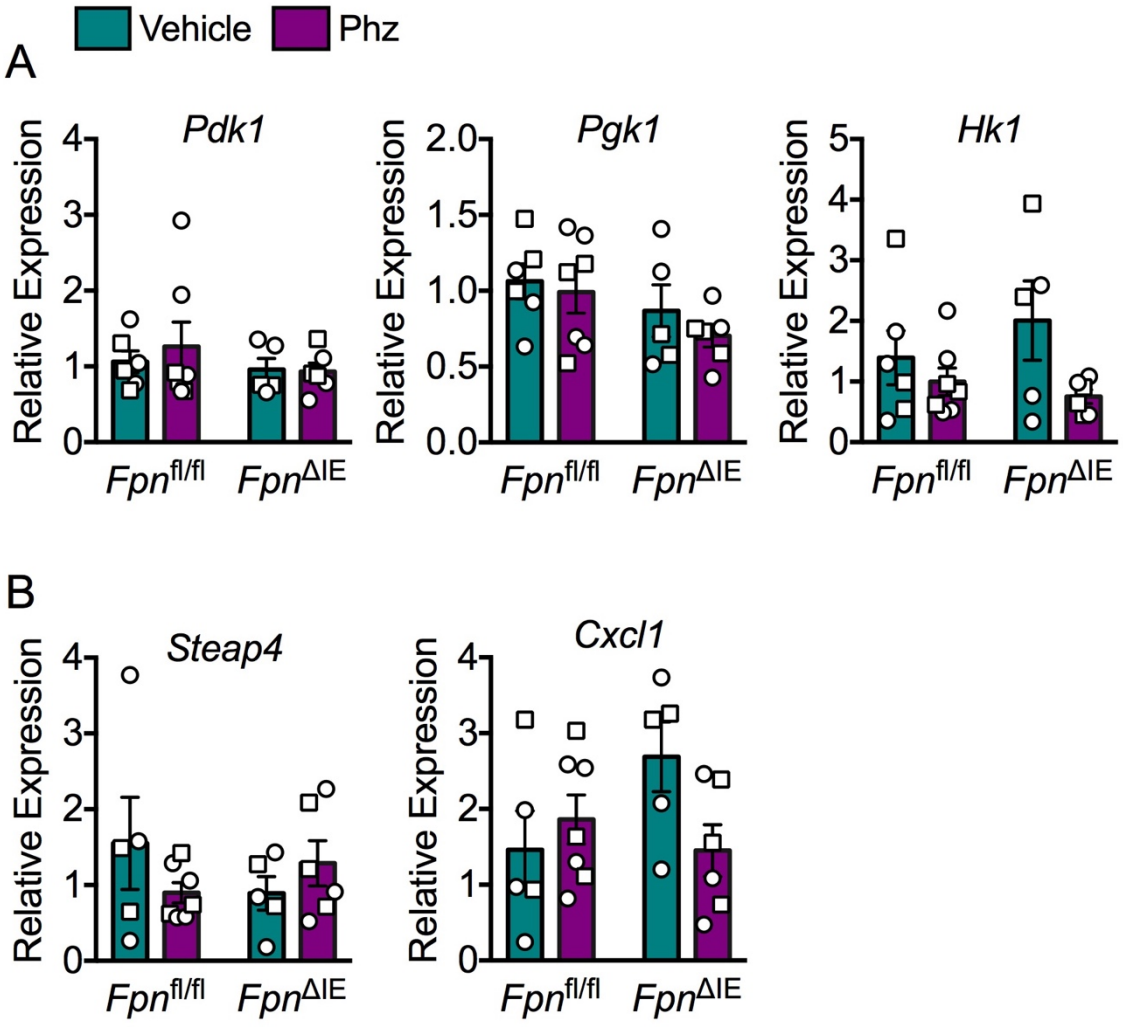

Supplemental Figure 4. Intestinal epithelial FPN does not mediate activation of intestinal HIF-1α or HIF-2α inflammatory targets in response to systemic erythropoietic demand. (**A**) qPCR analysis for HIF-1α-specific transcripts in duodenal samples (n = 5 to 6 per group). (**B**) qPCR analysis for HIF-2α-specific inflammatory transcripts in duodenal samples (n = 5 to 6 per group). Male samples are designated as squares and female samples are designated as circles. Mean ± SEM are plotted. Significance determined using two-way ANOVA with Tukey's post hoc.

Supplemental Figure 5.

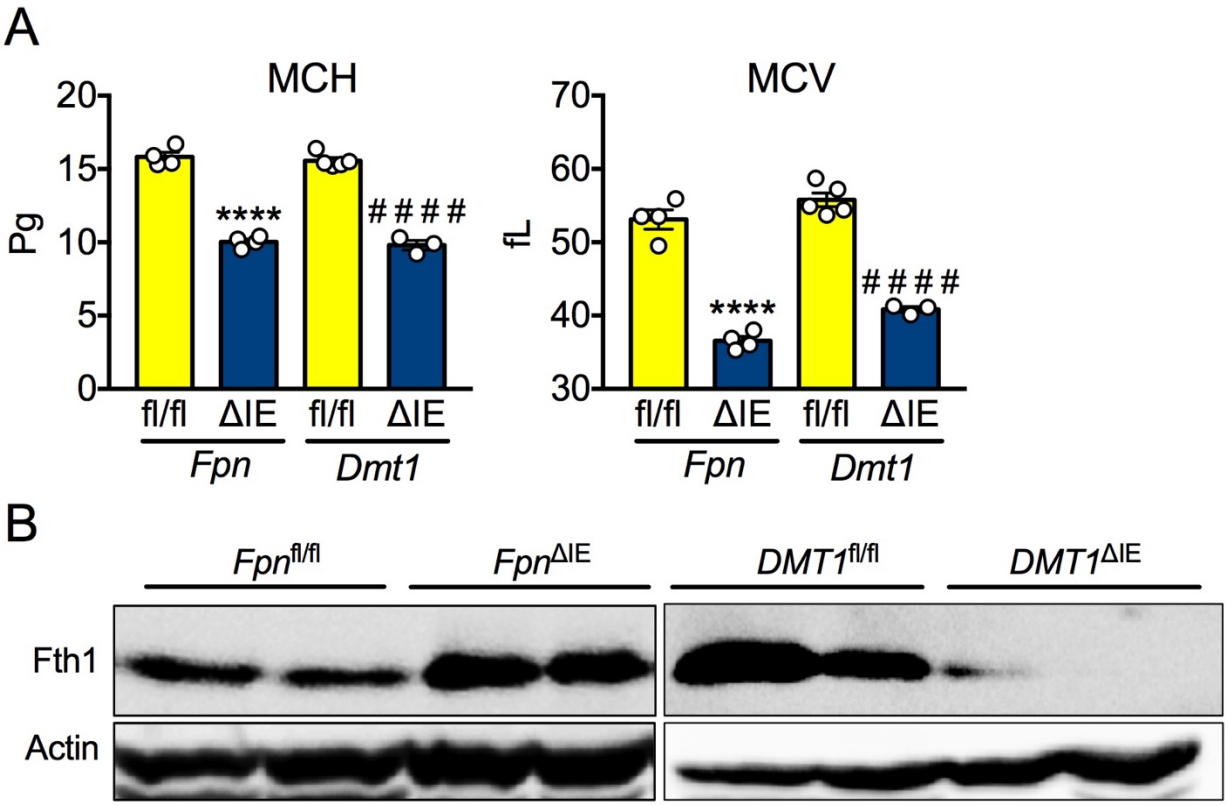

Supplemental Figure 5. Temporal deletion of FPN and DMT1 for three months both lead to iron-deficiency, microcytic and hypochromic anemia with differences in intestinal iron mobilization. (**A**) Analysis of mean corpuscular hemoglobin (MCH) and mean corpuscular volume (MCV) (n = 3 to 5 per group). (**B**) Western blot analysis for duodenal ferritin (FTH1) in *Fpn*$^{fl/fl}$, *Fpn*$^{\Delta IE}$, *Dmt1*$^{fl/fl}$, and *Dmt1*$^{\Delta IE}$ mice (n = 2 per group). Male samples are designated as squares and female samples are designated as circles. Mean ± SEM are plotted. Significance determined using 2-tailed unpaired t test. ****p < 0.0001 compared between *Fpn*$^{fl/fl}$ and *Fpn*$^{\Delta IE}$ cohorts. # # # #p < 0.0001 compared between *Dmt1*$^{fl/fl}$ and *Dmt1*$^{\Delta IE}$ cohorts.

Supplemental Figure 6.

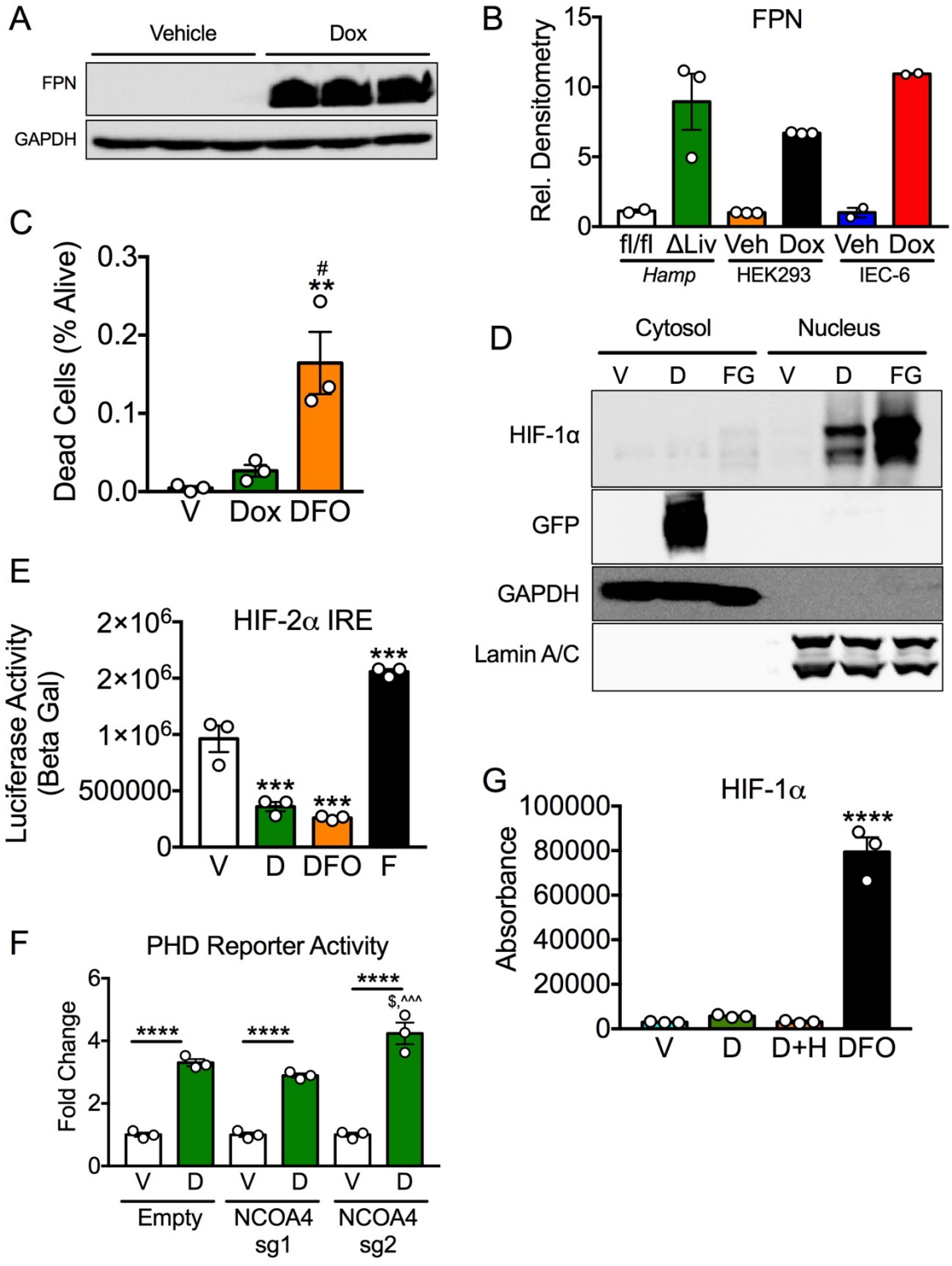

Supplemental Figure 6. Iron efflux through FPN is physiologically relevant and selective for HIF-2α. (**A**) Western blot analysis for FPN in FPN^{GFP} HEK293 cells treated with vehicle or 250 ng/mL doxycycline for 24-hours. (**B**) Relative densitometry to calculate fold induction of FPN protein in in vivo and in vitro models using data from Figure 1H, Figure 6I, and Supplemental Figure 6A. (**C**) Quantitation of dead cells using trypan blue following treatment of FPN^{GFP} HEK293 cells with doxycycline or 200 μM deferoxamine (DFO) for 48-hours. (**D**) Western blot analysis in cytosolic and nuclear fractions of FPN^{GFP} HEK293 cells treated with vehicle (V), doxycycline (D), or 100 μM FG4592 (FG) for 24-hours. (**E**) Relative luciferase activity in FPN^{GFP} HEK293 following treatment with vehicle (V), doxycycline (D), DFO, or 200 μM ferric ammonium citrate (FAC) (**F**). Fold change in luciferase activity in Empty, NCOA4 sg1, and NCOA4 sg2 FPN^{GFP} HEK293 cells infected with the PHD reporter and treated with doxycycline for 24-hours (**G**) ELISA in lysates from FPN^{GFP} IEC-6 cells treated with vehicle (V), doxycycline (D), doxycycline and 1mg/mL hepcidin (D+H), or DFO for 24-hours. Mean ± SEM are plotted. All cell culture experiments were repeated at least three times. Significance determined using one-way (**C, E, G**) or two-way (**F**) ANOVA with Tukey's post hoc. **p < 0.01; ***p < 0.001; ****p < 0.0001 compared to vehicle. #p < 0.05 compared to doxycycline. $p <0.05 compared to Empty doxycycline. ^^^p<0.001 compared to NCOA4 sg1 doxycycline.

Supplemental Figure 7.

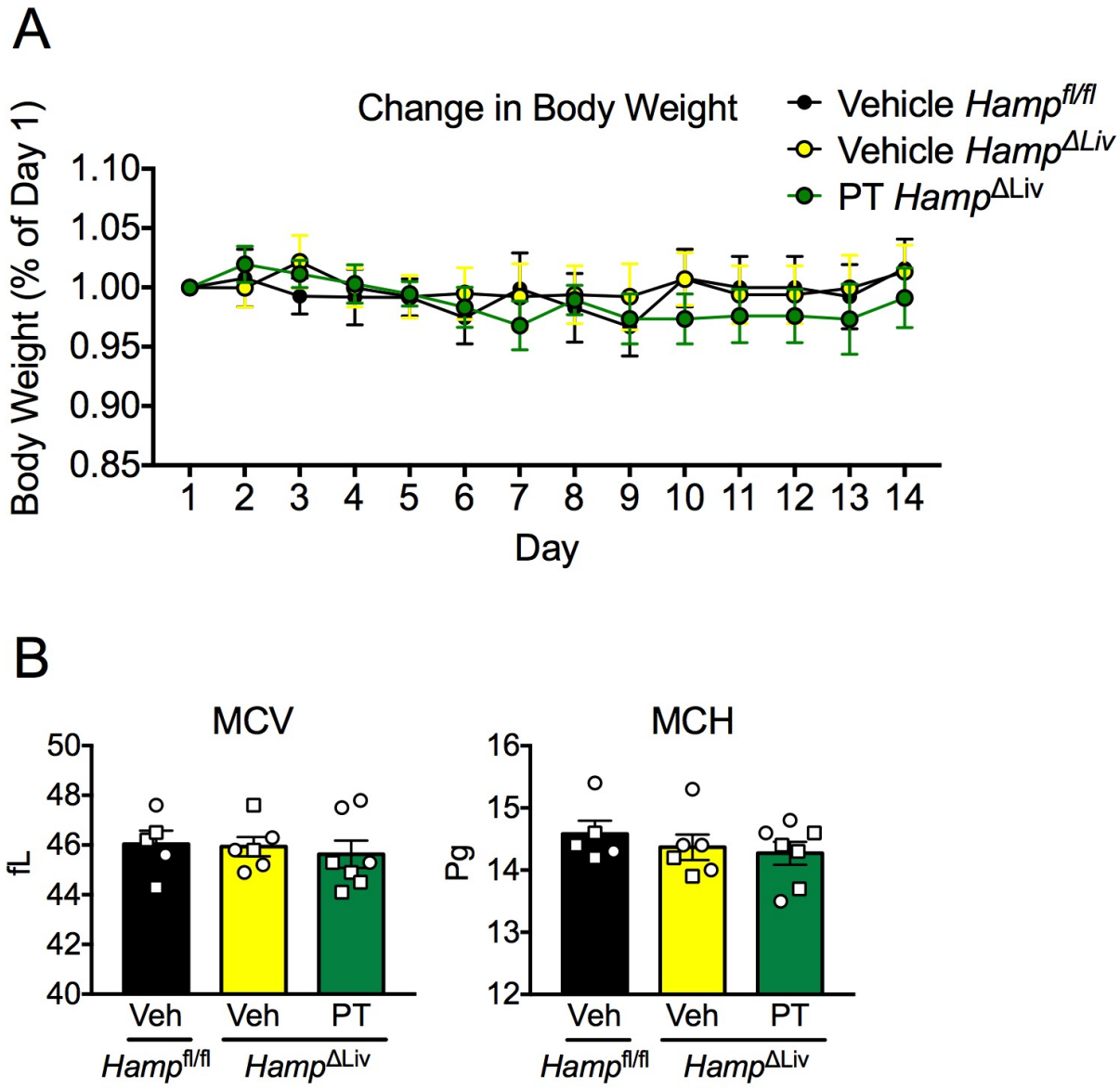

Supplemental Figure 7. Administration of PT2385 does not affect body weight or red blood cell size. (**A**) Body weight measurements of mice during two-week administration of either vehicle or PT2385 (n = 5 to 7 per group). (**B**) Analysis of mean corpuscular volume (MCV) and mean corpuscular hemoglobin (MCH) (n = 5 to 7 per group). Male samples are designated as squares and female samples are designated as circles. Mean ± SEM are plotted. Significance determined using one-way ANOVA with Tukey's post hoc.